Cell Host & Microbe
Article

IRSp53 Links the Enterohemorrhagic *E. coli* Effectors Tir and $EspF_U$ for Actin Pedestal Formation

Stefanie M. Weiss,[1,8] Markus Ladwein,[2,8] Dorothea Schmidt,[6] Julia Ehinger,[2] Silvia Lommel,[5] Kai Städing,[1] Ulrike Beutling,[4] Andrea Disanza,[7] Ronald Frank,[4] Lothar Jänsch,[3] Giorgio Scita,[7] Florian Gunzer,[6] Klemens Rottner,[2] and Theresia E.B. Stradal[1,*]

[1]Signalling and Motility Group
[2]Cytoskeleton Dynamics Group
[3]Cellular Proteomics Group
[4]Department of Chemical Biology
Helmholtz Centre for Infection Research, D-38124 Braunschweig, Germany
[5]University of Bonn, D-53121 Bonn, Germany
[6]Institute for Medical Microbiology and Hygiene, Faculty of Medicine Carl Gustav Carus, TU Dresden, 01307 Dresden, Germany
[7]IFOM Foundation, Institute FIRC of Molecular Oncology and University of Milan, School of Medicine, Dpt. San Paolo, 20139 Milan, Italy
[8]These authors contributed equally to this work
*Correspondence: theresia.stradal@helmholtz-hzi.de
DOI 10.1016/j.chom.2009.02.003

SUMMARY

Actin pedestal formation by pathogenic *E. coli* requires signaling by the bacterial intimin receptor Tir, which induces host cell actin polymerization mediated by N-WASP and the Arp2/3 complex. Whereas canonical enteropathogenic *E. coli* (EPEC) recruit these actin regulators through tyrosine kinase signaling cascades, enterohemorrhagic *E. coli* (EHEC) O157:H7 employ the bacterial effector $EspF_U$ (TccP), a potent N-WASP activator. Here, we show that IRSp53 family members, key regulators of membrane and actin dynamics, directly interact with both Tir and $EspF_U$. IRSp53 colocalizes with $EspF_U$ and N-WASP in actin pedestals. In addition, targeting of IRSp53 is independent of $EspF_U$ and N-WASP but requires Tir residues 454–463, previously shown to be essential for $EspF_U$-dependent actin assembly. Genetic and functional loss of IRSp53 abrogates actin assembly mediated by EHEC. Collectively, these data indentify IRSp53 family proteins as the missing host cell factors linking bacterial Tir and $EspF_U$ in EHEC pedestal formation.

INTRODUCTION

Gram-negative, Shiga toxin-producing enterohemorrhagic *E. coli* (EHEC) and the closely related enteropathogenic *E. coli* (EPEC) induce actin cytoskeleton rearrangements without invading their hosts (Hayward et al., 2006). Upon colonization of the intestinal mucosa, EPEC and EHEC strains cause ''attaching and effacing'' (A/E) lesions, which cause diarrhea in humans and animals. The A/E phenotype is characterized by intimate bacterial attachment to the epithelium, followed by a localized loss of microvilli (effacement) and the formation of pseudopod-like actin filament-filled structures underneath the bacteria, termed pedestals. In vitro, EPEC and EHEC are capable of inducing actin-rich pedestals in virtually every cell type, whereas in vivo, EPEC preferably affect the small intestine and EHEC affect the large intestine. Although morphologically indistinguishable, protein composition and molecular mechanism of formation of EPEC and EHEC pedestals are partly distinct (reviewed in Campellone and Leong, 2003). In our study, EPEC and EHEC refer to typical EPEC1 (strain 2348/69) and O157:H7 EHEC (strain EDL933), respectively, as commonly used model systems of actin rearrangements induced by these pathogens in vitro (Frankel and Phillips, 2008).

A/E lesion formation depends on bacterial virulence factors delivered into the host cell by a type III secretion system (TTSS), which is encoded on the locus of enterocyte effacement (LEE). The LEE also harbors the gene of the bacterial surface protein intimin and several translocated effector proteins, termed *E. coli*-secreted proteins (Esp), such as EspE, the intimin receptor also known as translocated intimin receptor (Tir). Upon Tir delivery and plasma membrane insertion, its interaction with intimin on the bacterial surface and clustering trigger signaling events that ultimately lead to actin pedestal formation (Campellone and Leong, 2003). Productive signaling to the actin cytoskeleton through Tir (but not firm attachment to the host) strictly depends on the presence of the host cell protein N-WASP (neural Wiskott-Aldrich syndrome protein) (Lommel et al., 2001, 2004). In spite of differences in N-WASP recruitment by EPEC versus EHEC-Tir, both pathogens exploit this host protein to drive Arp2/3 complex-mediated actin assembly. N-WASP is a ubiquitously expressed member of the WASP/Scar family of Arp2/3 complex activators that drives actin assembly, e.g., in endocytosis or vesicle-trafficking processes (Stradal and Scita, 2006). The C-terminal VCA domain of N-WASP directly binds actin and activates Arp2/3 complex (Rohatgi et al., 1999), and further N-terminal domains mediate subcellular positioning and/or autoregulation. Consequently, pedestal formation, but not N-WASP recruitment, depends on the presence of this VCA

domain in both EPEC (Lommel et al., 2001) and EHEC infections (Lommel et al., 2004).

EPEC and EHEC Tir differ concerning the mode of host protein recruitment. Upon binding to intimin, EPEC Tir is phosphorylated on tyrosine 474 (Kenny, 1999) by host family kinases (Phillips et al., 2004; Swimm et al., 2004). Although not entirely essential (Campellone and Leong, 2005), this phosphorylation is critical for EPEC-induced pedestal formation, as it provides a highly specific docking site for the cellular signaling adaptor protein Nck (Frese et al., 2006; Gruenheid et al., 2001), activating signaling pathways leading to actin assembly (Campellone et al., 2004a). In contrast, EHEC pedestal formation is independent of Tir tyrosine phosphorylation (DeVinney et al., 1999) and Nck (Gruenheid et al., 2001) but requires type III secretion-mediated delivery of an additional factor because EHEC Tir is unable to complement an EPEC Tir deletion mutant with regard to pedestal formation (DeVinney et al., 2001). The missing bacterial protein was independently identified by two laboratories and named $EspF_U$ or Tir cytoskeleton coupling protein (TccP) (Campellone et al., 2004b; Garmendia et al., 2004). $EspF_U$ is not encoded on the LEE but can be found on the cryptic prophage CP-933U in EHEC O157:H7, hence its name (*E. coli* secreted protein F-like from prophage U) (Campellone et al., 2004b). Interestingly, $EspF_U$/TccP was recently also found in the unusual EPEC strain O119:H6, and a highly homologous factor encoded by a gene absent in O157:H7, *tccP2*, can contribute to the actin polymerization pathway in atypical, sorbitol fermenting EHEC O157, most non-O157 EHEC, and in EPEC2 strains (Frankel and Phillips, 2008). $EspF_U$ comprises N-terminal sequences mediating type III secretion, probably aided by an unknown chaperone. The C terminus is composed of several highly conserved proline-rich repeats, 47 residues in length, the number of which can differ from 2.5 to 6.5 (Garmendia et al., 2005). These repeats bind to and activate N-WASP (Campellone et al., 2004b; Garmendia et al., 2004). Moreover, in spite of significant synergism observed for multiple $EspF_U$ repeats in inducing actin assembly (Campellone et al., 2008), each individual repeat can potently drive N-WASP activation through a hydrophobic segment, competing away the autoinhibitory C domain of N-WASP (Cheng et al., 2008; Sallee et al., 2008). In addition, N-WASP clustering was recently recognized to potentiate Arp2/3-mediated actin assembly (Padrick et al., 2008).

$EspF_U$ does not directly bind to Tir (Campellone et al., 2004b; Garmendia et al., 2004). Deletion studies revealed the region in Tir_{EHEC} essential for pedestal formation, encompassing residues 454–463 (Allen-Vercoe et al., 2006; Campellone et al., 2006) and also mediating indirect $EspF_U$ recruitment (Campellone et al., 2006). Because EHEC-Tir and $EspF_U$ are sufficient to drive pedestal formation of Tir-deficient EPEC or nonpathogenic *E. coli* (Campellone et al., 2004b, 2008), an as-yet unrecognized host cell factor must link Tir_{EHEC} to the $EspF_U$/N-WASP complex.

By using a combination of biochemical, proteomic, and cell biological approaches, we have identified this factor as the host protein IRSp53 (insulin receptor tyrosine kinase substrate p53). IRSp53 family proteins are well-established regulators of actin cytoskeleton reorganization at the plasma membrane and have previously been implicated in signaling to Arp2/3 complex-mediated actin polymerization via WASP/Scar family proteins (Scita et al., 2008; Takenawa and Suetsugu, 2007). Here, we show that IRSp53 proteins directly link Tir to the $EspF_U$/N-WASP complex, which is essential for actin pedestal formation induced by EHEC.

RESULTS

$EspF_U$ Repeats Bind Unknown Host Cell Linker Independently of N-WASP

The proline-rich repeats of $EspF_U$ (TccP) mediate interaction with N-WASP (Campellone et al., 2004b; Garmendia et al., 2006). Whereas each individual 47 residue repeat is capable of potently activating N-WASP in vitro, at least two repeats are required for efficient N-WASP-dependent actin assembly in vivo (Campellone et al., 2008; Cheng et al., 2008; Sallee et al., 2008). As N-terminal residues were shown to be required for $EspF_U$ translocation, but not for pedestal formation (Campellone et al., 2008; Garmendia et al., 2006), a full-length and an N-terminally truncated version of $EspF_U$ (Δ79, also termed ΔN) were employed for pull-down and cell-based assays (Figure 1A). $EspF_U$-ΔN readily coprecipitated N-WASP from fibroblast or brain tissue lysates (Figure 1B). In addition, GFP-tagged wild-type $EspF_U$ and $EspF_U$-ΔN were equally functional in reconstituting pedestal formation of $EspF_U$-deficient EHEC (Figure S1 available online), as expected (Figure 1C) (Campellone et al., 2008). Furthermore, both $EspF_U$ variants accumulated at bacteria/host cell interaction surfaces in the absence of N-WASP and, thus, actin reorganization (Figure 1D) (Lommel et al., 2004), similar to observations reported recently for full-length $EspF_U$ (Mousnier et al., 2008). These data confirmed $EspF_U$ accumulation to be separable from N-WASP binding and pedestal formation. They further established that the proline-rich repeats are dual function modules capable of both interaction with N-WASP and the unknown linker(s) recently proven to be of host cell origin (Campellone et al., 2008). Hence, $EspF_U$-ΔN emerged as a key candidate bait for enriching N-WASP-containing protein complexes operating in EHEC pedestal formation.

Characterization of N-WASP-Containing Protein Complexes Precipitated by $EspF_U$-ΔN

Ectopic expression of N-WASP and its hematopoietic homolog WASP can both reconstitute pedestal formation in N-WASP knockout cells (Lommel et al., 2004). Not surprisingly, therefore, both proteins were precipitated by $EspF_U$-ΔN from different cells and tissues (Figures 1E, S2A, and S2B). To test whether N-WASP/WASP bind to $EspF_U$ alone or in complex with one or more of its interaction partners, we probed $EspF_U$-ΔN pull-downs from different sources for the presence of selected interactors. In addition to N-WASP and WASP, $EspF_U$-ΔN pull-downs from mouse spleen also contained the WASP-interacting protein (WASPIP) family member WIP (Ho et al., 2004) and Arp2/3-complex (Figure S2B). It was reasonable to assume that both were coprecipitated through N-WASP/WASP and not through direct $EspF_U$ interactions, which was corroborated, e.g., by robust GFP-WIP precipitation in the presence, but not in the absence, of mRFP-N-WASP (Figure S2C). In addition, $EspF_U$-ΔN pull-downs did not contain coprecipitated cortactin or WAVE complex, as exemplified by the lack of the WAVE complex subunit Nap1 (Figure 1E). Although cortactin was proposed previously to interact with $EspF_U$ (Cantarelli et al., 2007), accumulation of $EspF_U$ in vivo was not sufficient for cortactin

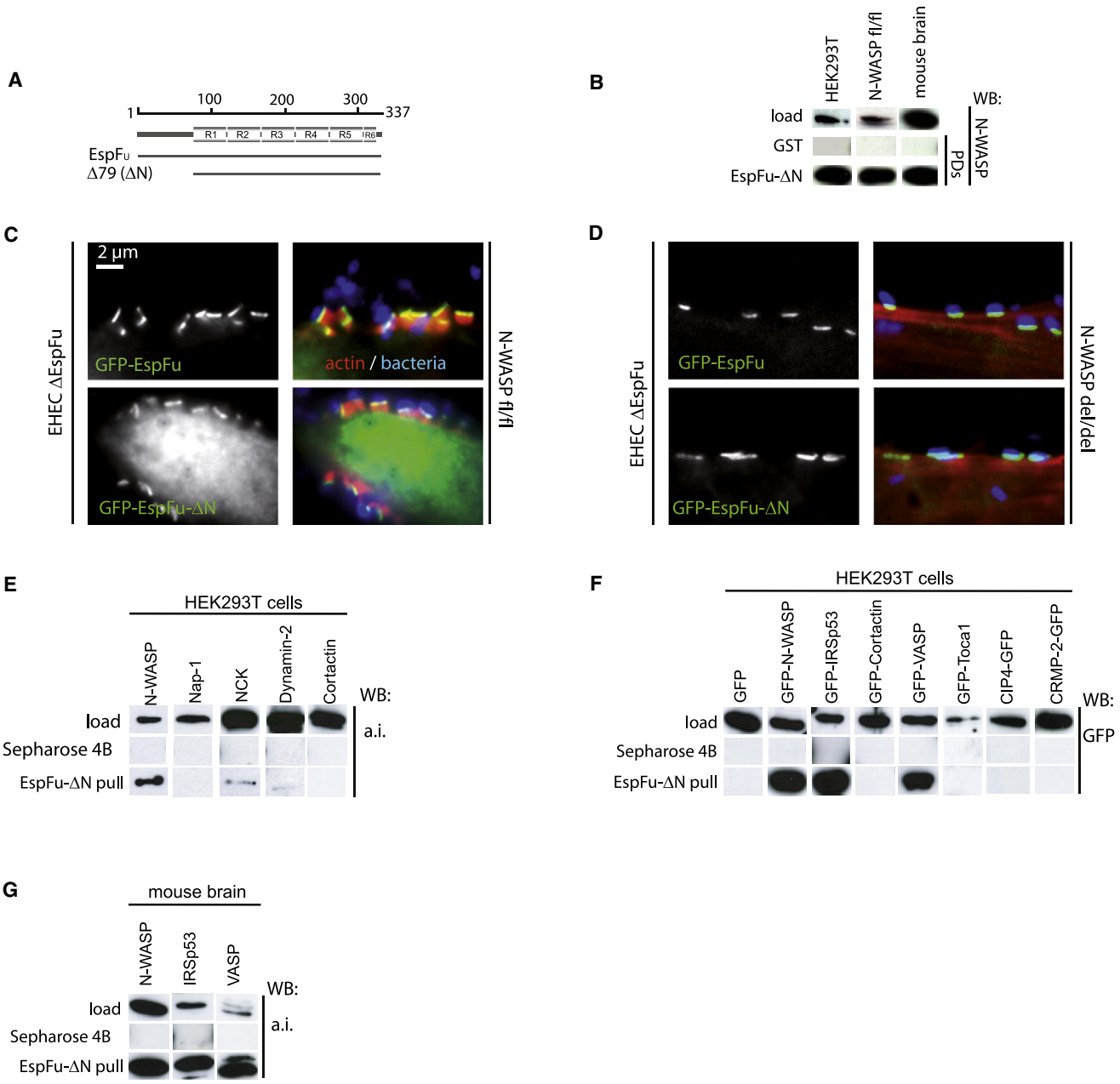

Figure 1. Characterization of $EspF_U$-ΔN Recruitment and Interactions

(A) Domain organization of $EspF_U$ and the ΔN variant used in this study.

(B) $EspF_U$-ΔN efficiently precipitates N-WASP from lysates of tissue culture cells (HEK293T and N-WASP fl/fl) or brain.

(C and D) GFP-tagged full-length $EspF_U$ or $EspF_U$-ΔN ectopically expressed in control (fl/fl) or N-WASP knockout (del/del) cells infected with EHEC$\Delta EspF_U$. Colors in merge correspond to lettering.

(E and F) Pull-downs of immobilized $EspF_U$-ΔN probed for the presence of different endogenous proteins (E) as indicated (a.i.) or GFP-tagged interaction candidates and GFP alone as control (F). Endogenous Nck and dynamin-2 may weakly be coprecipitated with N-WASP.

(G) $EspF_U$-ΔN precipitates from mouse brain extracts probed for endogenous IRSp53 and VASP.

recruitment to bacteria in the absence of N-WASP and actin pedestals (Mousnier et al., 2008), precluding a significant function for cortactin as $EspF_U$ interactor. Consistently, GFP-tagged cortactin was also not coprecipitated with $EspF_U$-ΔN (Figure 1F). The SH3-containing N-WASP activator Nck (Rohatgi et al., 1999) coprecipitated, albeit at low efficiency, perhaps through N-WASP (Figure 1E). Because Nck adaptors are relevant for EPEC, but not for EHEC, pedestal formation (Gruenheid et al., 2001), they are unlikely to link $EspF_U$ and Tir. Finally, dynamin 1 (data not shown) and 2, additional prominent N-WASP interactors implicated in pedestal formation (Unsworth et al., 2007), were coprecipitated only in minute amounts (Figure 1E).

Identification of $EspF_U$ Interactors

To identify new $EspF_U$ interactors that may link EHEC-Tir to N-WASP-dependent actin assembly, we separated samples from pull-downs using $EspF_U$-ΔN as bait by SDS-page and subjected them to mass spectrometry (Figure S3A). Significant hits repeatedly detected in samples from different tissues are listed in Tables S1 and S2. Apart from cortactin, dynamin, and WIP, mass spectrometry revealed promising candidates for linking Tir_{EHEC} and $EspF_U$. These included factors previously reported to play roles in cytoskeleton remodeling, such as CRMP-2, IRSp53, VASP, or the formin-binding protein 1 (FnBP1) family member Cip4 (Kwiatkowski et al., 2003; Scita et al., 2008; Tian et al., 2000). To confirm a specific interaction of these candidates with the $EspF_U$ repeat region, we performed pull-down assays from lysates of HEK293T cells ectopically expressing GFP-tagged proteins (Figure 1F). Though both GFP-IRSp53 and GFP-VASP were significantly enriched in the $EspF_U$-ΔN precipitate, no binding was detected for Cip4, the related Toca-1, or CRMP-2. The latter were excluded from further analyses, whereas precipitation of endogenous proteins, e.g., from mouse brain lysates, was confirmed for IRSp53 and VASP (Figure 1G). IRSp53 and Ena/VASP family members are also known to bind to each other (Krugmann et al., 2001; Scita et al., 2008), so these and their interactions with $EspF_U$ and Tir were explored in more detail. However, as VASP did not bind to the EHEC-Tir peptide essential for pedestal formation and recruiting $EspF_U$/N-WASP (see also Figure 3D), it cannot link Tir to the $EspF_U$/N-WASP complex (Figures S3B and S3C). Therefore, further experimentation focused on IRSp53 family members.

IRSp53 Targets to EHEC Independently of Both N-WASP and $EspF_U$

If singling out an individual factor capable of linking Tir_{EHEC} and $EspF_U$, this factor should bind to both $EspF_U$ and Tir. Moreover, its recruitment should be independent of N-WASP, which acts downstream of $EspF_U$. Finally, the interaction should be detectable for both Tir_{EHEC} and Tir_{EPEC} because previous domain swap experiments revealed the region of Tir linking to $EspF_U$/N-WASP recruitment and activation to be conserved among these Tir variants (Brady et al., 2007; Frankel and Phillips, 2008). We first tested whether GFP-tagged IRSp53 is recruited to bacterial attachment sites in both N-WASP control and knockout cells infected with either wild-type or $EspF_U$-deficient EHEC (Figure 2). GFP-IRSp53 was readily recruited to pedestal tips in N-WASP-expressing control cells (Figure 2A), coincident with $EspF_U$ and N-WASP accumulation (Campellone et al., 2004b; Lommel et al., 2004). IRSp53 was also prominently enriched in the absence of N-WASP and, thus, actin assembly (Figure 2A). To assess whether recruitment of IRSp53 to sites of EHEC attachment depends on the presence of either $EspF_U$ or N-WASP or both, we infected control and N-WASP knockout cells transfected with GFP-IRSp53 with $EspF_U$-deficient EHEC (Figure 2B). Strikingly, IRSp53 targeted to sites of EHECΔ$EspF_U$ attachment in both host cell types, showing that IRSp53 accumulation is independent of both N-WASP and $EspF_U$. To exclude that ectopically expressed GFP-tagged IRSp53 displayed activities different than the strictly regulated and autoinhibited endogenous protein (Disanza et al., 2006; Krugmann et al., 2001), we visualized both endogenous, translocated bacterial and host proteins in EHEC-infected epithelial cells (C127i). Monoclonal antibodies specific for Tir, IRSp53, $EspF_U$, and N-WASP all stained the pedestal tip (Figure 2C). Moreover, the same components except for $EspF_U$ were observed in EPEC-infected cells (Figure S4), demonstrating that both EPEC- and EHEC-Tir bind the potential linker IRSp53, as implicated previously (Brady et al., 2007; DeVinney et al., 2001). These results revealed that IRSp53 recruitment is upstream of $EspF_U$ and N-WASP signaling, potentially linking $EspF_U$/N-WASP to Tir in EHEC pedestal formation.

The SH3 Domain of IRSp53 Binds to the Proline-Rich Repeats in $EspF_U$

The modular IRSp53 has previously been reported to interact with numerous signaling or cytoskeletal regulators (reviewed in Scita et al., 2008), including N-WASP (Lim et al., 2008), so its enrichment in $EspF_U$ repeat pull-downs could have been explained by indirect interactions. To explore this further, we used GST-tagged full-length IRSp53, its isolated IMD, IMD plus central region (Δ364), or the isolated SH3 domain as baits in pull-down assays using $EspF_U$-ΔN as prey (for IRSp53 domain organization, see Figure 3A). Full-length IRSp53 and the isolated SH3 domain readily precipitated $EspF_U$-ΔN, whereas Δ364 and IMD both lacking SH3 did not (Figure 3B). To further narrow down the minimal binding surface for IRSp53 on $EspF_U$, we employed a set of $EspF_U$ variants harboring different numbers of repeats. All variants specifically coprecipitated with full-length IRSp53 or the isolated SH3 domain, but not with the IMD (Figure S5A), indicating that the SH3 domain can, in principle, bind to one proline-containing motif. To determine the interaction motif with IRSp53-SH3 within each 47-residue proline-rich repeat of $EspF_U$, we incubated an array of overlapping 15 mer peptides with GST-tagged IRSp53-SH3 and with the second and third SH3 domain of Nck1 as control. The array covered full-length $EspF_U$, as well as WIP and the proline-rich region of N-WASP (residues 271–390) (Table S3). Interestingly, IRSp53-SH3 recognized one specific motif in each $EspF_U$ repeat with the sequence IPPAPNWPAP. In this assay, IRSp53-SH3 did not significantly bind WIP or the spotted region of N-WASP, whereas Nck SH3 domains 2 and 3 interacted with WIP and N-WASP, respectively (Anton et al., 1998; Rohatgi et al., 2001), but not with $EspF_U$ (Figure 3C). Collectively, these data demonstrated a direct interaction of IRSp53-SH3 with each proline-rich repeat of $EspF_U$. However, coimmunoprecipitation experiments suggested increased binding efficiency with multiple $EspF_U$ repeats, at least in the context of a complex cellular environment (Figure S5B) and reminiscent of $EspF_U$-mediated N-WASP activation (Campellone et al., 2008; Cheng et al., 2008; Sallee et al., 2008). Consistently, as opposed to the GFP-tagged protein, endogenous N-WASP was not readily precipitated with one $EspF_U$ repeat (Figure S5C). We conclude that one $EspF_U$ repeat is not sufficient for effectively coupling IRSp53 to N-WASP-mediated actin assembly in vivo.

The IMD of IRSp53 Interacts with Tir of EPEC and EHEC

EPEC- and EHEC-Tir trigger a common, Nck-independent actin assembly pathway mediated by a core NPY motif, with the tyrosine located at positions 454 and 458 for EPEC and EHEC, respectively (Brady et al., 2007; Frankel and Phillips, 2008). To test whether IRSp53 constitutes the missing binding partner for this motif, we tested the C termini of both Tir_{EPEC} and Tir_{EHEC} (Figure 3D) or

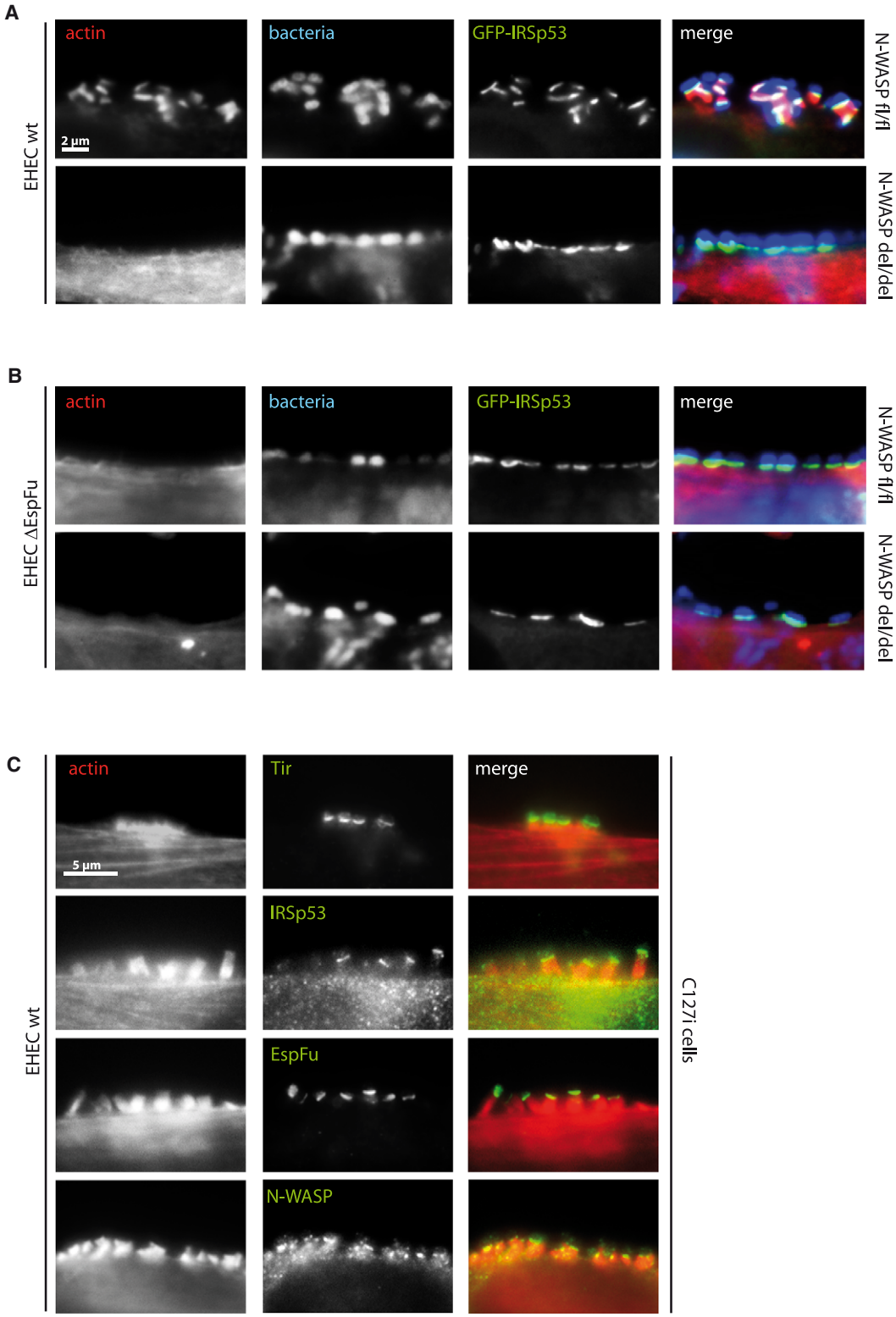

Figure 2. IRSp53 Is Recruited Upstream of Both N-WASP and $EspF_U$

(A and B) Fluorescence microscopy images showing N-WASP-expressing (fl/fl) or knockout (del/del) fibroblasts transfected with GFP-tagged IRSp53 and infected with wild-type or $EspF_U$-deficient EHEC ($\Delta EspF_U$) as indicated. IRSp53 is readily recruited to pedestal tips in the presence of N-WASP and $EspF_U$ (top panel) or to bacterial attachment sites in the absence of N-WASP, $EspF_U$, or both.

(C) Mouse epithelial C127i cells infected with EHEC stained for the actin cytoskeleton and translocated bacterial (Tir, $EspF_U$) or endogenous host proteins (N-WASP, IRSp53) as indicated.

$EspF_U$ as control for their ability to precipitate a set of ectopically expressed IRSp53 variants. Strikingly, both EPEC and EHEC Tir C termini precipitated all IRSp53 variants harboring its N-terminal IMD domain (Figure 3E). To confirm that the IMD of IRSp53 indeed interacts with the Tir regions located around the aforementioned NPY motif, we performed pull-downs with immobilized, short peptides corresponding to these regions (Figure 3D). Again, full-length IRSp53, its isolated IMD, and all variants harboring this domain were readily precipitated (Figure 3F). In contrast, the C terminus of Tir_{EHEC} did not interact with proline-rich repeats of $EspF_U$ (Figure 3G), as previously reported (Campellone et al., 2004b; Garmendia et al., 2004). Additional coimmunoprecipitation experiments confirmed a robust interaction of IRSp53 and the GFP-tagged C terminus of Tir_{EHEC} (Figure 3H). Moreover, interactions between Tir_{EHEC} and IRSp53-IMD, as well as the interaction of $EspF_U$-ΔN with IRSp53-SH3, were confirmed by using purified proteins (Figure S6A). Finally, pull-down assays using Tir peptides and lysates of N-WASP knockout cells transfected with GFP-tagged IRSp53 revealed a high-affinity interaction between Tir and IRSp53, as detected by Coomassie staining and subsequent mass spectrometric identification (Figure S6B).

Binding of IRSp53 to Tir Is Crucial for Pedestal Formation during EHEC Infection

Specific truncations of Tir_{EHEC} have previously been described to abolish actin pedestal formation (Allen-Vercoe et al., 2006; Campellone et al., 2006). A variant lacking almost the entire C terminus except for the aforementioned peptide region induced pedestals, whereas a mutant lacking 16 additional residues harboring the NPY motif did not (Figure 4A; Campellone et al., 2006). To explore whether these Tir variants coincided with differential IRSp53 and/or $EspF_U$ recruitment, we transformed EHEC strains genetically disrupted for wild-type Tir with the two Tir variants (TirΔ387–451 or TirΔ387–467) and used them for infections of C127i murine epithelial cells. EHEC-expressing TirΔ387–451 formed pedestals and recruited both endogenous IRSp53 and translocated $EspF_U$ to their tips (Figure 4B). The same was true for N-WASP (data not shown). In contrast, TirΔ387–467 neither induced pedestals nor mediated the enrichment of IRSp53 or $EspF_U$, although this Tir variant was inserted into the membrane and clustered beneath bacteria (Figure 4C). Therefore, residues 452–467 are decisive both for pedestal formation (Campellone et al., 2006) and for IRSp53 and $EspF_U$ recruitment.

Loss of IRSp53 Function Inhibits EHEC Pedestal Formation

To further explore the relevance of IRSp53 in Tir_{EHEC}-mediated and $EspF_U$-dependent pedestal formation, we utilized cells genetically deficient for IRSp53. IRSp53 KO cells stably transfected with mock plasmid or Flag-IRSp53 (Figure 5A) were infected with wild-type EHEC (Figure 5B, top panels) or EPEC (Figure 5B, bottom panels). Significantly, pedestal formation was observed in less than 5% of EHEC-infected cells, whereas re-expression of IRSp53 increased robust pedestal formation frequency over 10-fold to more than 50% (Figures 5B, top and 5C, left). Residual pedestal formation observed in IRSp53-deficient cells might be explained by low-level expression of the second IRSp53 family member IRTKS (insulin receptor tyrosine kinase substrate) (Figure S7) because this protein is recruited to sites of EHEC interaction in vivo and is able to bind to Tir and $EspF_U$ in vitro (Figure S8). The third family member, FLJ22852, which is absent in our cell lines (data not shown), also bound $EspF_U$, but not Tir (Figure S8), indicating functions in EHEC pedestal formation to be restricted to the two broadly expressed family members, IRSp53 and IRTKS. As opposed to EHEC, EPEC pedestal formation was observed in roughly 90% of both IRSp53 knockout and reconstituted cells (Figures 5B, bottom and 5C, right), suggesting that at least in the presence of the EPEC-specific Tir-Y474- and Nck-dependent pathway to N-WASP signaling (Campellone et al., 2004a; Gruenheid et al., 2001), IRSp53 is not necessary for pedestal formation. Importantly, IRSp53 operates in $EspF_U$ and N-WASP recruitment downstream of EHEC-Tir, as IRSp53 KO cells failed to accumulate both proteins below attached wild-type EHEC, in contrast to the clear $EspF_U$ and N-WASP targeting observed in the same cells re-expressing Flag-IRSp53 (Figure S9).

The IMD and SH3 Domain of IRSp53 Are Both Essential for $EspF_U$-Dependent Pedestal Formation

To reveal the relevance of different IRSp53 domains in EHEC pedestal formation in more detail in vivo, we subjected IRSp53-deficient cells re-expressing mutated or truncated versions of the protein to EHEC infections (summarized in Figure 6B). Full-length, GFP-IRSp53 readily reconstituted pedestal formation and localized to the actin membrane interface at pedestal tips (Figure 6A, top and data not shown). A point mutation causing a nonfunctional SH3 domain (IRSp53ΔSH3) that cannot bind, e.g., to its prominent interactor Eps8 (Disanza et al., 2006), as well as two C-terminally deleted variants (Δ364 lacking residues 365–521 and Δ250 comprising only the N-terminal IMD) were prominently recruited to sites of Tir clustering beneath attached bacteria but failed to induce pedestal formation (Figure 6A, middle panels). Finally, the C-terminal fragment harboring the SH3 domain (residues 365–521) did not even localize to sites of bacterial attachment and failed to restore actin assembly, as would be expected if the N-terminal IMD is required for linking IRSp53 to Tir. These data show that both IMD and SH3 of IRSp53 are required for linking Tir to the $EspF_U$/N-WASP complex in EHEC actin pedestal formation.

Membrane and Actin Filament Binding of IRSp53 Are Dispensable for Pedestal Formation

The IMD of IRSp53 family proteins was previously described to mediate membrane binding and deformation or actin binding and bundling (reviewed in Scita et al., 2008). These activities could also influence pedestal formation induced by EHEC, in addition to or inseparable from operating as an essential linker protein. Thus, we compared pedestal formation induced by wild-type IRSp53 and a variant, four arginines of which (at positions 142, 143, 146, and 147) had been mutated to glutamic acid (IRSp53[4KE]) (Millard et al., 2005). Mutation of these residues did not interfere with dimerization, as expected (Suetsugu et al., 2006; Figure S10A). Unexpectedly, however, IRSp53[4KE] prominently supported EHEC-induced pedestal formation (Figure 6A, bottom; for quantification, see Figure 6C). Consistently, IMD domains harboring the same mutations ([4KE]-IMD) were precipitated by Tir-derived peptides in a manner

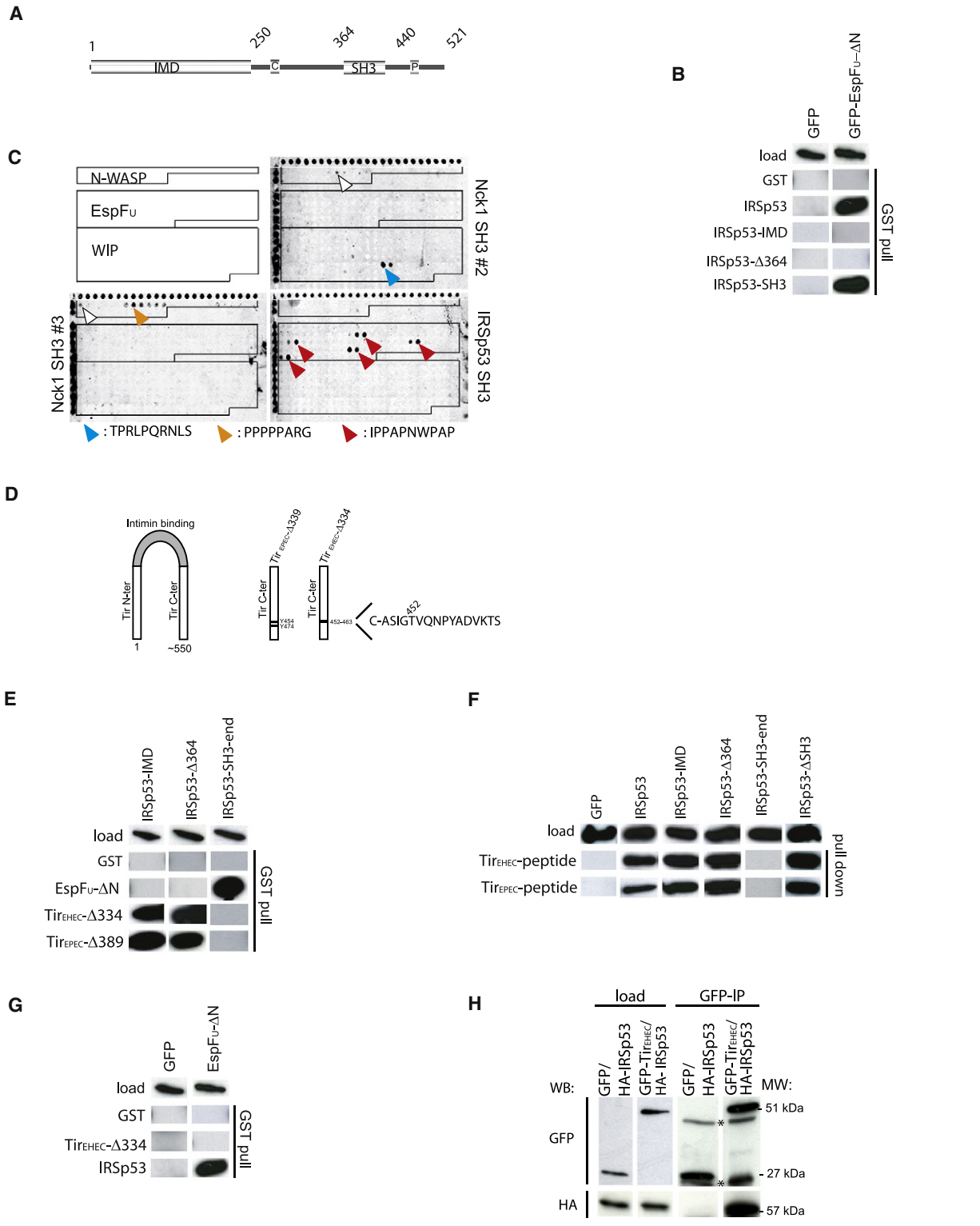

Figure 3. IRSp53 Interacts Directly with $EspF_U$ and Tir

(A) Domain organization of IRSp53.

(B) Pull-down experiments with GST-tagged full-length IRSp53 or different truncation mutants from lysates of HEK293T cells transfected with GFP-tagged $EspF_U$-ΔN or GFP alone as control.

(C) Overlay assays with the second and third SH3 domains of Nck1 or that of IRSp53 on an array of peptides representing the proline-rich region of N-WASP (aa 271–390), full-length $EspF_U$, and full-length WIP as depicted on the top left. Respective SH3 domains predominantly bound to spots corresponding to peptide

indistinguishable to wild-type IMD (Figure S10B). Likewise, full-length WT and IRSp53[4KE] could both be precipitated with Tir_{EHEC}, Tir_{EPEC}, and $EspF_U$-ΔN (Figure S10C), showing that the function of IRSp53 in linking Tir and $EspF_U$ was not significantly altered by the 4KE mutation. Although it is difficult to entirely exclude that membrane deformation and/or F-actin binding activities of IRSp53 contribute, to some extent, to pedestal formation, these activities are certainly not essential. Instead, we conclude the predominant function of IRSp53 and, presumably, IRTKS to constitute the missing host cell factor linking the two bacterial proteins Tir and $EspF_U$. Such a scenario is confirmed by recruitment and complete abolishment of EHEC pedestal formation solely through moderate expression of GFP-IMD, apparently interrupting the signaling pathway to $EspF_U$/N-WASP-dependent actin assembly (Figure S11).

DISCUSSION

$EspF_U$ has a dual function in EHEC-mediated pedestal formation downstream of the bacterial effector Tir. First, it directly binds to and activates N-WASP during pedestal formation, and second, it contributes to N-WASP recruitment to the bacterial attachment site through at least one unknown host cell factor. In this study, we set out to identify this missing link between the bacterial attachment receptor Tir_{EHEC} and the $EspF_U$/N-WASP signaling complex.

We first confirmed that the proline-rich repeats of $EspF_U$ used for subsequent pull-down experiments were sufficient to restore $EspF_U$ functions and to link to Tir independently of N-WASP interactions (Campellone et al., 2006, 2008; Mousnier et al., 2008). $EspF_U$ repeats ($EspF_U$-ΔN) were employed for large-scale pull-down experiments and subsequent mass spectrometry. Pull-downs were performed in actin assembly conditions, requiring stringent criteria for selection and ranking of candidate linkers (for candidate lists, see Tables S1 and S2). Considerations included previous reports on involvement in pedestal formation, N-WASP-dependent processes, or more general types of actin assembly. Table S2 lists candidate proteins that were analyzed further. Most initial, promising candidates were dropped upon more detailed experimentation. For instance, an important role in pedestal formation induced by pathogenic *E. coli* was recently ascribed to cortactin, a Tir interactor and relevant Arp2/3 complex activator (Cantarelli et al., 2006) that we had also identified in our pull-downs (Tables S1 and S2). However, unlike N-WASP, neither EGFP-tagged cortactin nor the endogenous protein coprecipitated with $EspF_U$ repeats from lysates of cells (Figures 1E and 1F), speaking against an essential function in Tir_{EHEC}-induced targeting of $EspF_U$/N-WASP-dependent actin polymerization. Moreover, cortactin was described to interact with the N terminus of Tir (Cantarelli et al., 2007), a domain involved in the regulation of pedestal length, whereas the region required for pedestal formation was recently confined to 10 residues located in the C terminus of Tir_{EHEC} (Allen-Vercoe et al., 2006; Campellone et al., 2006). Similar results were obtained for dynamins. Thus, as suggested for cortactin recently (Mousnier et al., 2008), we conclude that both cortactin and dynamin could modulate Arp2/3-dependent actin assembly in pedestals downstream of N-WASP recruitment. Likewise, WIP family proteins appeared to coprecipitate with $EspF_U$ repeats only through indirect interaction via N-WASP, disqualifying them as likely linkers of Tir and $EspF_U$.

Ena/VASP proteins, which had been implicated in EPEC and EHEC pedestal formation previously (Goosney et al., 2000, 2001), prominently interacted with $EspF_U$ but failed to bind Tir. These proteins, which can also bind IRSp53 (Scita et al., 2008), may thus promote actin assembly at pedestal tips by means other than linking the two bacterial proteins. One hit repeatedly appearing in our MS analyses was Cip4/Trip10, which is a member of the formin-binding protein 1 (Fnbp1) family also comprising Fnbp1/FBP17 and the N-WASP-binding protein Fnbp1L/Toca-1 (Ho et al., 2004; Itoh et al., 2005). However, neither Cip4 nor Toca-1 bound to $EspF_U$ or to Tir_{EHEC} in subsequent high stringency experiments in which N-WASP was still clearly enriched.

We then turned to the analysis of the BAIAP2 (brain-specific angiogenesis inhibitor 1 associated protein 2) family of proteins (Yamagishi et al., 2004), comprising IRSp53, IRTKS, and FLJ22582. The overall domain organization of this protein family is reminiscent of, but not identical to, the Fnbp1 family proteins, with a BAR-related N-terminal IM (IRSp53 and MIM homologous) domain (IMD) involved in membrane deformation and F-actin binding (Scita et al., 2008). The more C-terminal SH3 domain was shown to interact with various actin regulators, e.g., the Arp2/3 complex activator WAVE2 (Miki et al., 2000) that cannot mediate Arp2/3 complex activation in pedestals (Lommel et al., 2004), but also with Eps8 (Disanza et al., 2006) or Ena/VASP proteins (Krugmann et al., 2001).

Our experiments clearly uncover the minimal requirements to link EHEC-Tir to N-WASP-mediated actin polymerization and pedestal formation and pinpoint IRSp53 as the missing factor (see also Figure 7 for a summary of interaction for all components of the pathway). This signaling cascade starts off from a C-terminal motif in Tir_{EHEC}, previously established to correspond to residues 454–563 (Allen-Vercoe et al., 2006; Campellone et al., 2006), which bind to the N-terminal IMD of IRSp53, which, in turn—via its C-terminal SH3 domain—binds to the proline-rich repeats of

motifs as indicated. Arrowheads are color coded: orange, Nck1-SH3 #3; blue, Nck-1 SH3 #2; red, IRSp53-SH3. Nck-SH3 domains also showed weak binding to one related motif (white arrowheads). For a complete list of peptides and their binding properties, see Table S3.

(D) Overview of the bacterial Tir-receptor and the two N-terminally deleted Tir constructs (EPEC and EHEC) used in this study.

(E) Lysates of HEK293T cells transfected with different GFP-tagged IRSp53 fragments were subjected to pull-downs with GST alone, GST-tagged $EspF_U$-ΔN, or the C termini of Tir_{EHEC} and Tir_{EPEC}.

(F) Precipitates of EPEC-Tir-derived and EHEC-Tir-derived peptides (Tir_{EPEC}: C-ATSSAVVNPYAEVGEA; Tir_{EHEC}: C-ASIGTVQNPYADVKTS) immobilized on CNBr Sepharose from lysates of cells expressing different GFP-tagged IRSp53 variants.

(G) Lack of direct binding between Tir_{EHEC} and $EspF_U$-ΔN as revealed by Tir_{EHEC}-Δ334 pull-downs from lysates of cells expressing GFP-$EspF_U$ repeats. GST alone served as negative control, and IRSp53 served as positive control. Blots in (E)–(G) were probed with anti-GFP antibodies.

(H) Coimmunoprecipitation of GFP-tagged Tir_{EHEC} C terminus and HA-IRSp53 using anti-GFP antibodies (GFP-IP) (right lane, bottom). Asterisks indicate heavy and light chains of the antibody used in the IP.

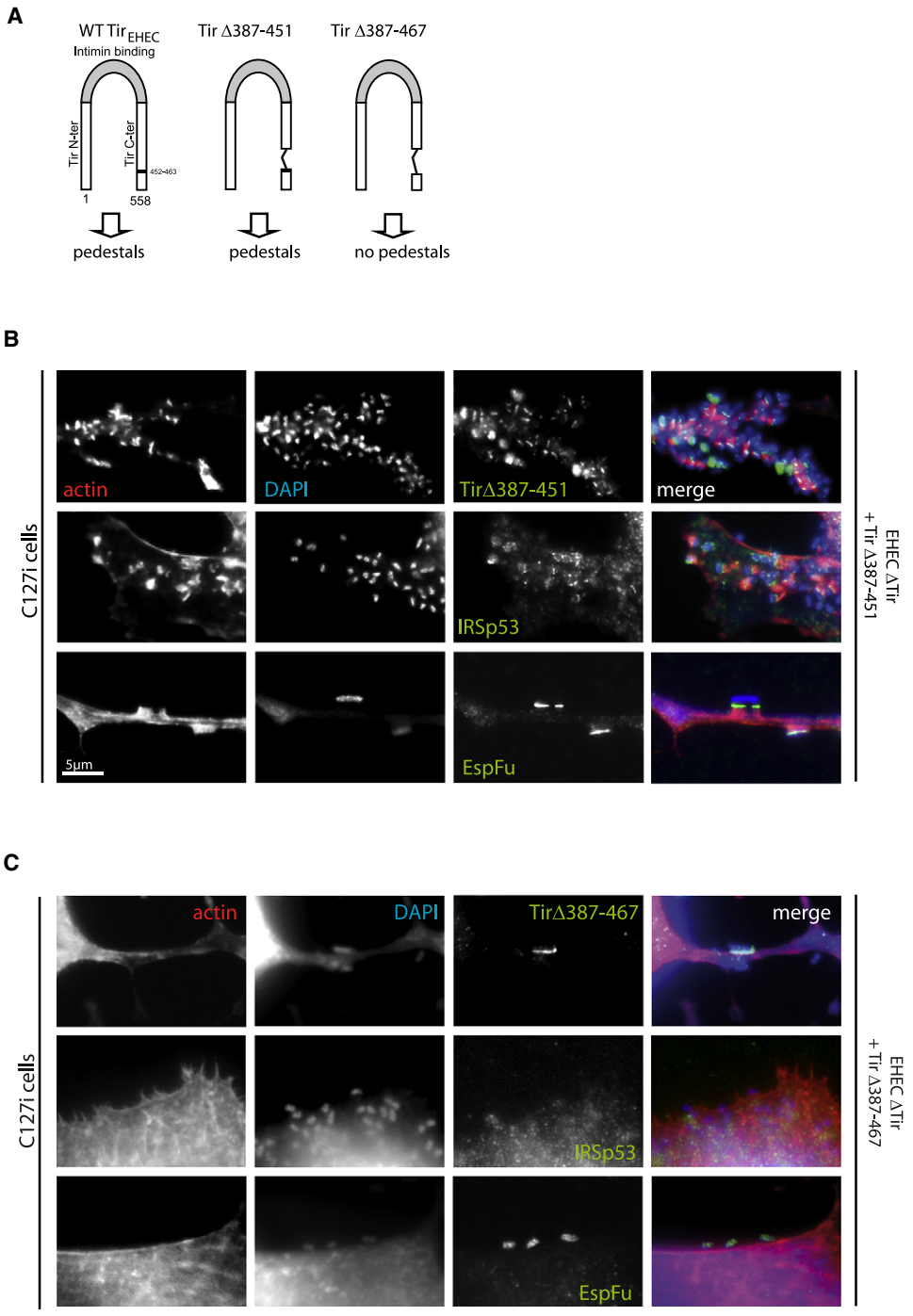

Figure 4. A Small, C-Terminal Tir Fragment Is Decisive for IRSp53 Recruitment and Pedestal Formation

(A) Schematic overview of the Tir variants used and their established effects on EHEC-induced pedestal formation.

(B and C) C127i cells infected with Tir-deficient EHEC re-expressing the Tir variants shown in (A) and stained for actin, IRSp53, or $EspF_U$. Note that, in the absence of IRSp53 recruitment (C), $EspF_U$ is not detected as an accumulation at sites of bacteria/host cell interaction but instead weakly labels the entire bacteria.

$EspF_U$/TccP. Furthermore, the same repeats also bind the autoinhibitory motif in N-WASP, allowing potent activation of the latter and, thus, of Arp2/3 complex-mediated actin assembly (Cheng et al., 2008; Daugherty-Clarke and Goode, 2008; Sallee et al., 2008).

Interestingly, IRSp53 is a dimer (Millard et al., 2005). The two N termini of IRSp53 associate in an antiparallel fashion to form a functional IMD, which may harbor one or two binding sites for Tir. Consequently, two IRSp53 SH3 domains may signal to at least two times five (in our case) $EspF_U$ proline-rich repeats,

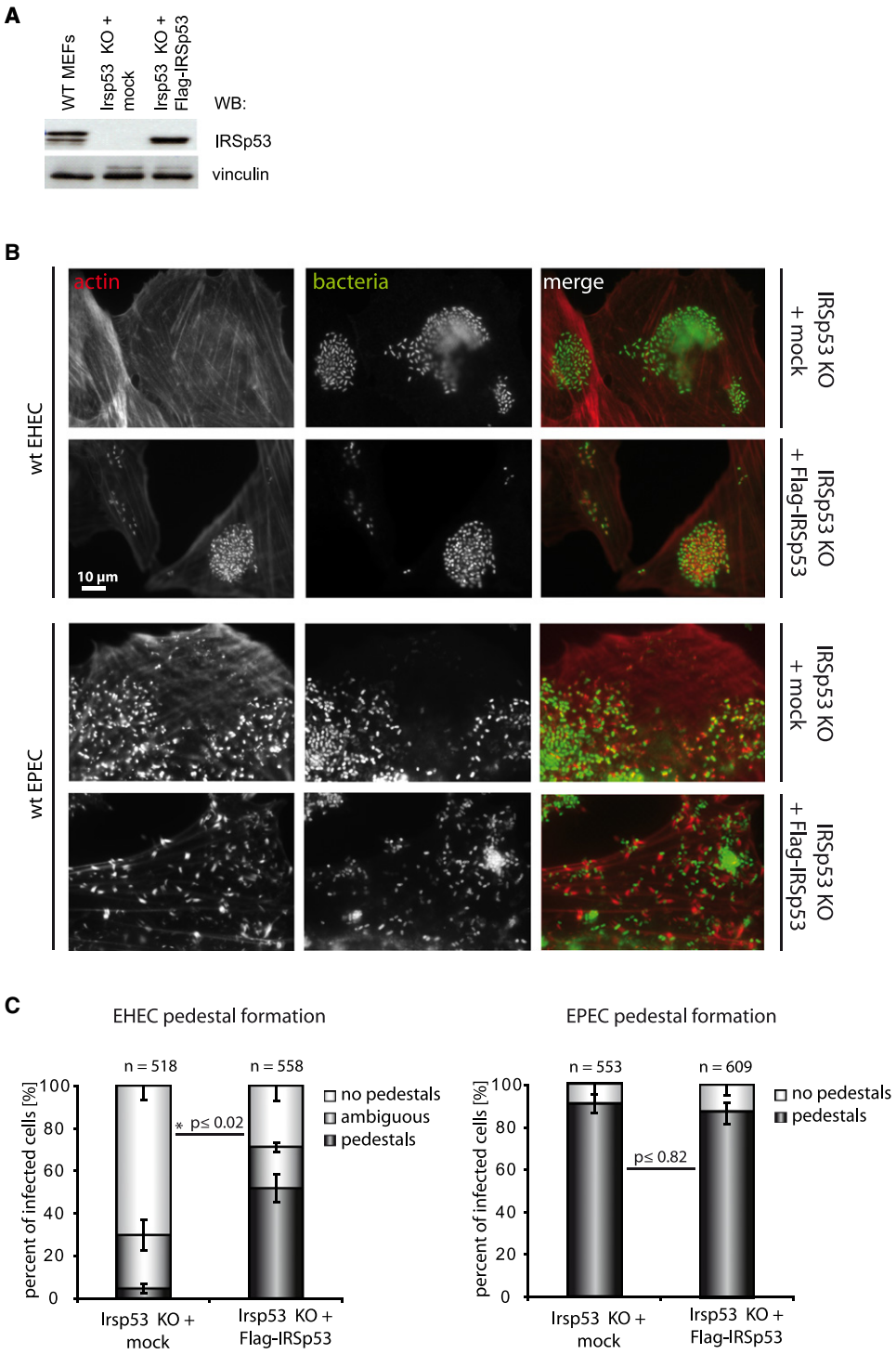

Figure 5. Loss of IRSp53 Function Abrogates EHEC, but Not EPEC, Pedestal Formation

(A) IRSp53 expression in embryonic wild-type fibroblasts (WT MEFs) as compared to IRSp53 KO cells mock transfected or re-expressing Flag-tagged IRSp53. Vinculin served as loading control.

(B) Infection experiments with EHEC or EPEC in IRSp53 KO or reconstituted cells as indicated.

(C) Quantification of pedestal formation from experiments as shown in (B) (see also Table S4). Data are arithmetic means and standard errors of means (SEMs, error bars) from three independent experiments. n is the total number of cells analyzed. Data were statistically compared by using two-sample t test, with a significant difference confirmed for EHEC, but not EPEC.

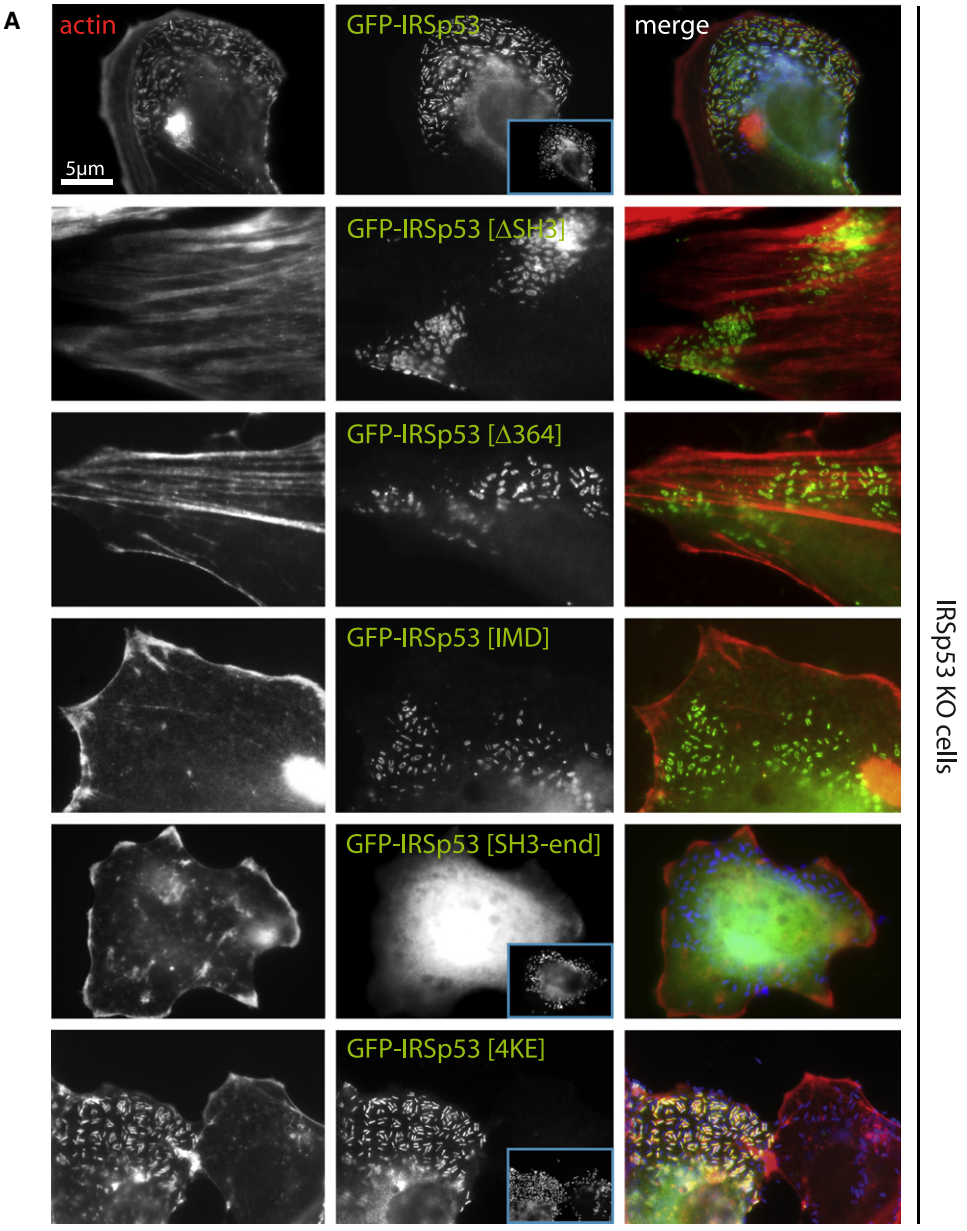

B

	localization beneath bacteria	pedestal formation
IRSp53	+++	+++
IRSp53ΔSH3	+++	-
Δ364	+++	-
IMD	+++	-
SH3-end	-	-
IRSp53 [4KE]	+++	+++

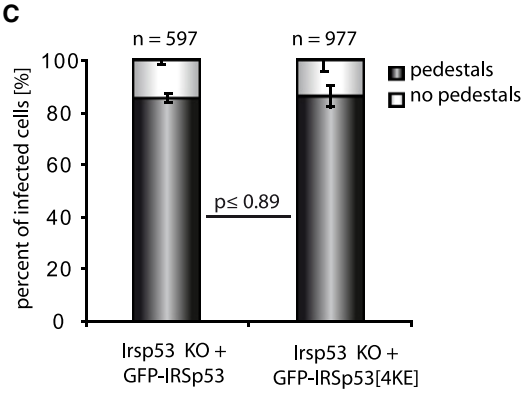

each capable of activating N-WASP molecules in a synergistic fashion (Campellone et al., 2008). Thus, IRSp53 may serve as a bona fide signal amplification platform (Figure 7D). A better understanding of how Tir and IMDs associate precisely may only come from cocrystallization.

Complementary experimental approaches causing defective IRSp53 recruitment all confirmed the significance of these proteins for connecting Tir_{EHEC} to $EspF_U$/N-WASP because lack of their accumulation consistently abolished EHEC pedestal formation (see, e.g., Figures 4, 5, 6, and S11).

In summary, we report a signaling cascade composed of alternating bacterial and host cell factors designed to transduce and amplify signals elicited by bacterial Tir receptors to drive actin nucleation by the N-WASP/Arp2/3 complex. We uncover IRSp53 family proteins as the missing physical link between Tir and the $EspF_U$/N-WASP complex. Our data add an exciting new twist to the multitude of functions established for IRSp53 family proteins in both membrane- and actin-remodeling events.

EXPERIMENTAL PROCEDURES

cDNA Cloning, Expression Constructs, and Antibodies

The sequence encoding full-length $EspF_U$ (TccP) was obtained by PCR on EHEC (enterohemorrhagic *E. coli* 0157:H7). The derived cDNA was ligated into pCR4-Topo Blunt (Invitrogen). The resulting construct corresponded to an $EspF_U$ variant harboring 5.5 repeats, the sequence of which had been deposited (NC_002695). All further $EspF_U$ constructs used in this study were either derived from this cDNA or synthesized (Genescript) and subcloned into pEGFP-C (Clontech, Palo Alto) or pGEX6-P (GE Healthcare) vectors. All variants of the IRSp53 family and CRMP-2 were cloned by PCR amplification or restriction digest using EGFP-IRSp53 or IMAGE clones BC015459, BC015619, and BC067109 as templates, respectively, and subcloned as for $EspF_U$. All constructs were sequence verified. PCR primers are given in Table S5, and additional expression constructs and antibodies are given in the Supplemental Data.

Bacterial Strains

Strains used in this study were enteropathogenic *E. coli* strain E2348/69 (O127:H6) (Levine et al., 1978), enterohemorrhagic *E. coli* strain 86-24 (O157:H7) (Griffin et al., 1988), and enterohemorrhagic *E. coli* strain EDL933 (O157:H7) (BCCM 15068/ATCC 43895). A knockout mutation of the *$espF_U$* gene in O157:H7 EHEC EDL 933 was obtained as described in the Supplemental Data. The EHEC strain genetically deficient for *tir* (EHECΔTir) and reconstitution constructs mediating expression of HA-tagged Tir-Δ387–451 and Tir-Δ387–467 were kindly provided by John Leong (Campellone et al., 2006).

Cells and Transfections

N-WASP control (fl/fl) and knockout (del/del) fibroblasts were as described (Lommel et al., 2001). For immunolocalization studies, cells were plated on glass coverslips coated with 25 μg/ml fibronectin (Roche) prior to infection and fixation as indicated. HEK293T cells (ATCC CRL-11268), B16-F1 mouse melanoma cells (ATCC CRL-6323), mouse mammary gland epithelial cells C127i (ATCC CRL-1616), and HeLa (ATCC CCL-2) were grown in RPMI 1640 (for HEK293T) or DMEM 4.5 g/l glucose (Invitrogen) supplemented with 10% FBS (PAA, Germany), 2 mM glutamine, and 50 U/ml Penicillin/Streptomycin (Invitrogen). Transfections were carried out with FuGENE 6 (Roche, Mannheim, Germany) or Superfect (for HEK293T, QIAGEN, Germany), according to manufacturer's protocols. IRSp53-deficient cells were spontaneously immortalized fibroblasts prepared from homozygous E14 embryos of a mouse carrying a GeneTrap insertion (Bay Genomics: ES cell clone Accession Number XG757). Preparation and characterization of these, as well as Flag-IRSp53-reconstituted cells, will be described elsewhere (A.D. and G.S., unpublished data).

Immunofluorescence

EPEC and EHEC infections were performed as described (Campellone et al., 2006; Lommel et al., 2004). For fluorescence microscopy, cells were fixed with 4% formaldehyde (PFA) in PBS for 20 min followed by permeabilization with a mixture of 0.1% Triton X-100 and PFA for 45 s. Alexa dye-labeled secondary reagents and phalloidin were from Invitrogen. Fluorescence microscopy and image acquisition were as described (Lommel et al., 2004). Images were processed with Metamorph (Universal Imaging) and Photoshop CS2 (Adobe).

Immunoprecipitations and Pull-Down Assays

For immunoprecipitations, cells grown in 10 cm diameter dishes were washed with PBS, lysed in 500 μl of ice-cold lysis buffer (8 mM Tris base, 12 mM HEPES [pH 7.5], 50 mM NaCl, 15 mM KCl, 3 mM $MgCl_2$, 1% Triton X-100, and EDTA-free protease inhibitor cocktail Complete Mini [Roche, Germany]) for 20 min on ice. Tissues were washed in ice-cold PBS and homogenized in a Dounce homogenizer with 1 volume/weight of tissue lysis buffer (20 mM HEPES [pH 7.5], 50 mM NaCl, 1 mM $MgCl_2$, 1 mM EGTA, 0.2 mM $CaCl_2$, 1 mM DTE, 0.5 mM ATP, 20 mM NaF, and 1 mM $NaVO_3$). Homogenates from cells and tissues were centrifuged for 45 min at 15.000 × g. Cleared lysates were snap frozen in liquid nitrogen for storage. For immunoprecipitations or pull-downs, lysates were incubated with the respective antibodies as indicated for 2 hr, followed by incubation with protein G Sepharose beads (Amersham Biosciences) for 1 hr at 4°C on a rotary wheel. Beads were washed with lysis buffer and processed for western blot analysis. For pull-downs, recombinant GST-tagged proteins were expressed and purified following standard protocols (GE Healthcare) and immobilized on glutathione Sepharose beads at 2–5 mg protein/ml slurry in PBS (10 mM $NaPO_4$ [pH 7.5], 150 mM NaCl, supplemented with 1 mM DTE, protease inhibitor cocktail, and 10% glycerol), snap frozen, and stored at −70°C. Alternatively, GST was cleaved off using PreScission Protease (GE Healthcare). Proteins were purified further using a MonoQ ion exchange column (GE Healthcare) and covalently coupled to CNBr-activated Sepharose 4B (GE Healthcare, Germany) according to the manufacturer's protocol. Beads were processed as described above. For pull-downs, cell or tissue lysates were incubated with 30 μl of slurry for 1 hr at 4°C on a rotary wheel. Samples were washed three times with the respective lysis buffer, resolved on SDS-PAGE, and either processed for mass spectrometry (see below) or resolved and analyzed by immunoblotting. Peptide overlays were performed as described (Beutling et al., 2008).

Mass Spectrometry

Prominent individual bands or groups of less prominent bands as judged from colloidal Coomassie-stained gels (Westermeier et al., 1997) were excised and treated with a slightly modified method of Shevchenko (Shevchenko et al., 2000). Proteins were identified with MALDI-TOF MS and ESI-MS/MS essentially as described (Trost et al., 2005). PMF data and MS/MS fragmentation data were analyzed with an internal MASCOT server (version 1.9; Matrix Science, London, UK) (Perkins et al., 1999) searching against the NCBI

Figure 6. IRSp53-IMD and IRSp53-SH3 Are Both Essential for Linking Tir_{EHEC} to Actin Assembly

(A) IRSp53 KO cells re-expressing the GFP-tagged IRSp53 variants as listed in (B) were subjected to EHEC infections and examined for the actin cytoskeleton (red in merges) and IRSp53-variant localization (green in merges). Boxed insets show bacteria stained with anti-Tir antibodies (blue in merges). IRSp53 variants harboring the IMD domain are recruited, and those harboring both the IMD and SH3 domains are able to reconstitute pedestal formation in IRSp53 KO cells (see also categorization in [B]). The SH3 domain is not recruited to sites of bacterial attachment. The bar is valid for all images except insets.

(B) Summary of results shown in (A).

(C) Quantification and statistics of EHEC pedestal formation in infected cells expressing GFP-tagged wild-type IRSp53 versus the 4KE mutant. Data are arithmetic means and standard errors of means (SEMs, error bars) from three independent experiments. n is the total number of cells analyzed (see also Table S4). Reconstitution of pedestal formation by wild-type or 4KE-IRSp53 was not statistically different, as confirmed by two-sample t test.

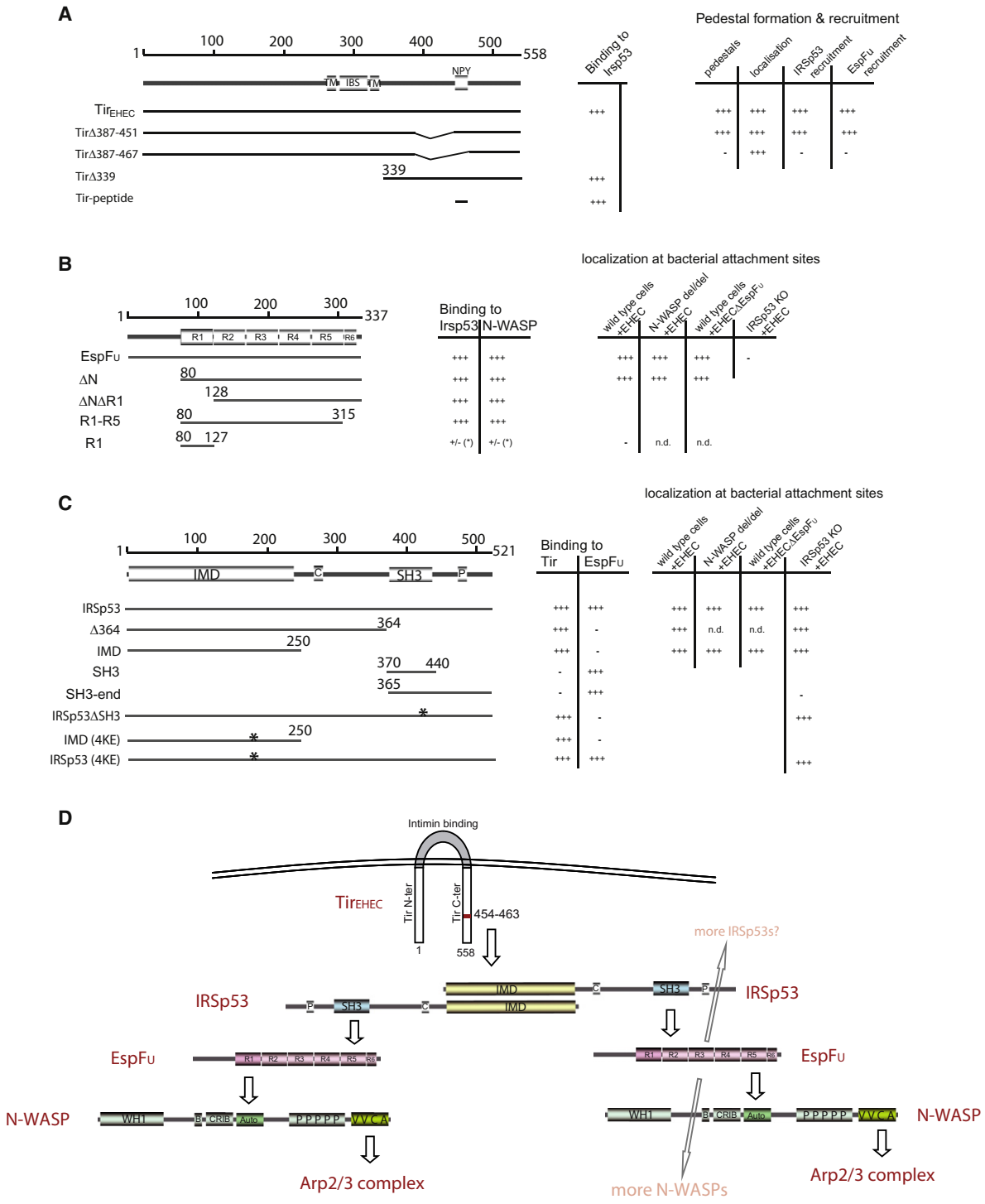

Figure 7. Data Summary and Resulting Model for EHEC Pedestal Formation

(A) EHEC-Tir variants and corresponding functional data concerning their IRSp53 binding or their abilities to cluster below bacteria or to mediate pedestal formation or IRSp53 and $EspF_U$ recruitment.

(B) $EspF_U$ and employed fragments, a summary of their binding capabilities to IRSp53 and N-WASP (center), and their abilities to localize to Tir in different infection conditions (right).

(C) Domain structure of IRSp53 and used fragments and a summary of their interactions with $EspF_U$ or Tir and of their recruitment in vivo.

(D) Model of proposed signal transduction pathway from Tir_{EHEC} to Arp2/3 complex-mediated actin polymerization during pedestal formation. Functional IMDs of IRSp53 are dimers; hence, two SH3 domains of the IRSp53 dimer potentially recruit two $EspF_U$ molecules and, in turn, multiple N-WASP molecules, allowing efficient and highly clustered Arp2/3 complex activation to drive focal actin assembly. Further signal amplification may derive from recruitment of additional IRSp53 molecules through multiple $EspF_U$ repeats. Arrow, more IRSp53s.

database. The criteria used to accept protein identifications based on PMF data included the extent of sequence coverage, the number of peptides matched (minimum of 5), and the score of probability (minimum of 60 for the MOWSE score). For a list of identified proteins, including score and sequence coverage values, see Table S1.

SUPPLEMENTAL DATA

Supplemental Data include Supplemental Experimental Procedures, 11 figures, and 6 tables and can be found with this article online at http://www.cell.com/cell-host-microbe/supplemental/S1931-3128(09)00065-1.

ACKNOWLEDGMENTS

We are grateful to Brigitte Denker, Petra Hagendorff, Kirsten Minkhart, and Dr. Manfred Nimtz for expert technical assistance and for mass spectrometric measurements. We also thank Frank Ebel (Munich) for kindly providing anti-Tir antibodies and Sohail Ahmed (Singapure), Anke Fabian (Münster), Hiroyuki Nakagawa (Fukuoka), Ed Schuuring (Groningen), and Roger Tsien (La Jolla) for expression constructs. We are also grateful to John Leong (Worcester) for providing EHEC strains and Tir constructs and for invaluable discussions during the course of this study. This work was supported by grants from the German Research Council (DFG) to T.E.B.S. (FOR471 and SPP1150), K.R. (SFB621), and F.G. (SFB621). L.J. was supported by EU NoE grant EuroPathoGenomics (LSHB-CT-2005-512061). A.D. is supported by a FIRC fellowship, and G.S. is supported by a grant of the Italian Association for Cancer Research (AIRC).

Received: March 8, 2008
Revised: December 30, 2008
Accepted: February 11, 2009
Published: March 18, 2009

REFERENCES

Allen-Vercoe, E., Waddell, B., Toh, M.C., and DeVinney, R. (2006). Amino acid residues within enterohemorrhagic Escherichia coli O157:H7 Tir involved in phosphorylation, alpha-actinin recruitment, and Nck-independent pedestal formation. Infect. Immun. *74*, 6196–6205.

Anton, I.M., Lu, W., Mayer, B.J., Ramesh, N., and Geha, R.S. (1998). The Wiskott-Aldrich syndrome protein-interacting protein (WIP) binds to the adaptor protein Nck. J. Biol. Chem. *273*, 20992–20995.

Beutling, U., Stading, K., Stradal, T., and Frank, R. (2008). Large-scale analysis of protein-protein interactions using cellulose-bound peptide arrays. Adv. Biochem. Eng. Biotechnol. *110*, 115–152.

Brady, M.J., Campellone, K.G., Ghildiyal, M., and Leong, J.M. (2007). Enterohaemorrhagic and enteropathogenic Escherichia coli Tir proteins trigger a common Nck-independent actin assembly pathway. Cell. Microbiol. *9*, 2242–2253.

Campellone, K.G., and Leong, J.M. (2003). Tails of two Tirs: Actin pedestal formation by enteropathogenic E. coli and enterohemorrhagic E. coli O157:H7. Curr. Opin. Microbiol. *6*, 82–90.

Campellone, K.G., and Leong, J.M. (2005). Nck-independent actin assembly is mediated by two phosphorylated tyrosines within enteropathogenic Escherichia coli Tir. Mol. Microbiol. *56*, 416–432.

Campellone, K.G., Rankin, S., Pawson, T., Kirschner, M.W., Tipper, D.J., and Leong, J.M. (2004a). Clustering of Nck by a 12-residue Tir phosphopeptide is sufficient to trigger localized actin assembly. J. Cell Biol. *164*, 407–416.

Campellone, K.G., Robbins, D., and Leong, J.M. (2004b). EspFU is a translocated EHEC effector that interacts with Tir and N-WASP and promotes Nck-independent actin assembly. Dev. Cell *7*, 217–228.

Campellone, K.G., Brady, M.J., Alamares, J.G., Rowe, D.C., Skehan, B.M., Tipper, D.J., and Leong, J.M. (2006). Enterohaemorrhagic Escherichia coli Tir requires a C-terminal 12-residue peptide to initiate EspF-mediated actin assembly and harbours N-terminal sequences that influence pedestal length. Cell. Microbiol. *8*, 1488–1503.

Campellone, K.G., Cheng, H.C., Robbins, D., Siripala, A.D., McGhie, E.J., Hayward, R.D., Welch, M.D., Rosen, M.K., Koronakis, V., and Leong, J.M. (2008). Repetitive N-WASP-binding elements of the enterohemorrhagic Escherichia coli effector EspF(U) synergistically activate actin assembly. PLoS Pathog. *4*, e1000191.

Cantarelli, V.V., Kodama, T., Nijstad, N., Abolghait, S.K., Iida, T., and Honda, T. (2006). Cortactin is essential for F-actin assembly in enteropathogenic Escherichia coli (EPEC)—and enterohaemorrhagic E. coli (EHEC)—induced pedestals and the α-helical region is involved in the localization of cortactin to bacterial attachment sites. Cell. Microbiol. *8*, 769–780.

Cantarelli, V.V., Kodama, T., Nijstad, N., Abolghait, S.K., Nada, S., Okada, M., Iida, T., and Honda, T. (2007). Tyrosine phosphorylation controls cortactin binding to two enterohaemorrhagic Escherichia coli effectors: Tir and EspFu/TccP. Cell. Microbiol. *9*, 1782–1795.

Cheng, H.C., Skehan, B.M., Campellone, K.G., Leong, J.M., and Rosen, M.K. (2008). Structural mechanism of WASP activation by the enterohaemorrhagic E. coli effector EspF(U). Nature *454*, 1009–1013.

Daugherty-Clarke, K., and Goode, B.L. (2008). WASp identity theft by a bacterial effector. Dev. Cell *15*, 333–334.

DeVinney, R., Stein, M., Reinscheid, D., Abe, A., Ruschkowski, S., and Finlay, B.B. (1999). Enterohemorrhagic Escherichia coli O157:H7 produces Tir, which is translocated to the host cell membrane but is not tyrosine phosphorylated. Infect. Immun. *67*, 2389–2398.

DeVinney, R., Puente, J.L., Gauthier, A., Goosney, D., and Finlay, B.B. (2001). Enterohaemorrhagic and enteropathogenic Escherichia coli use a different Tir-based mechanism for pedestal formation. Mol. Microbiol. *41*, 1445–1458.

Disanza, A., Mantoani, S., Hertzog, M., Gerboth, S., Frittoli, E., Steffen, A., Berhoerster, K., Kreienkamp, H.J., Milanesi, F., Di Fiore, P.P., et al. (2006). Regulation of cell shape by Cdc42 is mediated by the synergic actin-bundling activity of the Eps8-IRSp53 complex. Nat. Cell Biol. *8*, 1337–1347.

Frankel, G., and Phillips, A.D. (2008). Attaching effacing Escherichia coli and paradigms of Tir-triggered actin polymerization: Getting off the pedestal. Cell. Microbiol. *10*, 549–556.

Frese, S., Schubert, W.D., Findeis, A.C., Marquardt, T., Roske, Y.S., Stradal, T.E., and Heinz, D.W. (2006). The phosphotyrosine peptide binding specificity of Nck1 and Nck2 Src homology 2 domains. J. Biol. Chem. *281*, 18236–18245.

Garmendia, J., Phillips, A.D., Carlier, M.F., Chong, Y., Schuller, S., Marches, O., Dahan, S., Oswald, E., Shaw, R.K., Knutton, S., et al. (2004). TccP is an enterohaemorrhagic Escherichia coli O157:H7 type III effector protein that couples Tir to the actin-cytoskeleton. Cell. Microbiol. *6*, 1167–1183.

Garmendia, J., Frankel, G., and Crepin, V.F. (2005). Enteropathogenic and enterohemorrhagic Escherichia coli infections: Translocation, translocation, translocation. Infect. Immun. *73*, 2573–2585.

Garmendia, J., Carlier, M.F., Egile, C., Didry, D., and Frankel, G. (2006). Characterization of TccP-mediated N-WASP activation during enterohaemorrhagic Escherichia coli infection. Cell. Microbiol. *8*, 1444–1455.

Goosney, D.L., DeVinney, R., Pfuetzner, R.A., Frey, E.A., Strynadka, N.C., and Finlay, B.B. (2000). Enteropathogenic E. coli translocated intimin receptor, Tir, interacts directly with alpha-actinin. Curr. Biol. *10*, 735–738.

Goosney, D.L., DeVinney, R., and Finlay, B.B. (2001). Recruitment of cytoskeletal and signaling proteins to enteropathogenic and enterohemorrhagic Escherichia coli pedestals. Infect. Immun. *69*, 3315–3322.

Griffin, P.M., Ostroff, S.M., Tauxe, R.V., Greene, K.D., Wells, J.G., Lewis, J.H., and Blake, P.A. (1988). Illnesses associated with Escherichia coli O157:H7 infections. A broad clinical spectrum. Ann. Intern. Med. *109*, 705–712.

Gruenheid, S., DeVinney, R., Bladt, F., Goosney, D., Gelkop, S., Gish, G.D., Pawson, T., and Finlay, B.B. (2001). Enteropathogenic E. coli Tir binds Nck to initiate actin pedestal formation in host cells. Nat. Cell Biol. *3*, 856–859.

Hayward, R.D., Leong, J.M., Koronakis, V., and Campellone, K.G. (2006). Exploiting pathogenic Escherichia coli to model transmembrane receptor signalling. Nat. Rev. Microbiol. *4*, 358–370.

Ho, H.Y., Rohatgi, R., Lebensohn, A.M., Le, M., Li, J., Gygi, S.P., and Kirschner, M.W. (2004). Toca-1 mediates Cdc42-dependent actin nucleation by activating the N-WASP-WIP complex. Cell *118*, 203–216.

Itoh, T., Erdmann, K.S., Roux, A., Habermann, B., Werner, H., and De Camilli, P. (2005). Dynamin and the actin cytoskeleton cooperatively regulate plasma membrane invagination by BAR and F-BAR proteins. Dev. Cell *9*, 791–804.

Kenny, B. (1999). Phosphorylation of tyrosine 474 of the enteropathogenic Escherichia coli (EPEC) Tir receptor molecule is essential for actin nucleating activity and is preceded by additional host modifications. Mol. Microbiol. *31*, 1229–1241.

Krugmann, S., Jordens, I., Gevaert, K., Driessens, M., Vandekerckhove, J., and Hall, A. (2001). Cdc42 induces filopodia by promoting the formation of an IRSp53:Mena complex. Curr. Biol. *11*, 1645–1655.

Kwiatkowski, A.V., Gertler, F.B., and Loureiro, J.J. (2003). Function and regulation of Ena/VASP proteins. Trends Cell Biol. *13*, 386–392.

Levine, M.M., Bergquist, E.J., Nalin, D.R., Waterman, D.H., Hornick, R.B., Young, C.R., and Sotman, S. (1978). Escherichia coli strains that cause diarrhoea but do not produce heat-labile or heat-stable enterotoxins and are non-invasive. Lancet *1*, 1119–1122.

Lim, K.B., Bu, W., Goh, W.I., Koh, E., Ong, S.H., Pawson, T., Sudhaharan, T., and Ahmed, S. (2008). The Cdc42 effector IRSp53 generates filopodia by coupling membrane protrusion with actin dynamics. J. Biol. Chem. *283*, 20454–20472.

Lommel, S., Benesch, S., Rottner, K., Franz, T., Wehland, J., and Kuhn, R. (2001). Actin pedestal formation by enteropathogenic Escherichia coli and intracellular motility of Shigella flexneri are abolished in N-WASP-defective cells. EMBO Rep. *2*, 850–857.

Lommel, S., Benesch, S., Rohde, M., Wehland, J., and Rottner, K. (2004). Enterohaemorrhagic and enteropathogenic Escherichia coli use different mechanisms for actin pedestal formation that converge on N-WASP. Cell. Microbiol. *6*, 243–254.

Miki, H., Yamaguchi, H., Suetsugu, S., and Takenawa, T. (2000). IRSp53 is an essential intermediate between Rac and WAVE in the regulation of membrane ruffling. Nature *408*, 732–735.

Millard, T.H., Bompard, G., Heung, M.Y., Dafforn, T.R., Scott, D.J., Machesky, L.M., and Futterer, K. (2005). Structural basis of filopodia formation induced by the IRSp53/MIM homology domain of human IRSp53. EMBO J. *24*, 240–250.

Mousnier, A., Whale, A.D., Schuller, S., Leong, J.M., Phillips, A.D., and Frankel, G. (2008). Cortactin recruitment by enterohemorrhagic Escherichia coli O157:H7 during infection in vitro and ex vivo. Infect. Immun. *76*, 4669–4676.

Padrick, S.B., Cheng, H.C., Ismail, A.M., Panchal, S.C., Doolittle, L.K., Kim, S., Skehan, B.M., Umetani, J., Brautigam, C.A., Leong, J.M., et al. (2008). Hierarchical regulation of WASP/WAVE proteins. Mol. Cell *32*, 426–438.

Perkins, D.N., Pappin, D.J., Creasy, D.M., and Cottrell, J.S. (1999). Probability-based protein identification by searching sequence databases using mass spectrometry data. Electrophoresis *20*, 3551–3567.

Phillips, N., Hayward, R.D., and Koronakis, V. (2004). Phosphorylation of the enteropathogenic E. coli receptor by the Src-family kinase c-Fyn triggers actin pedestal formation. Nat. Cell Biol. *6*, 618–625.

Rohatgi, R., Ma, L., Miki, H., Lopez, M., Kirchhausen, T., Takenawa, T., and Kirschner, M.W. (1999). The interaction between N-WASP and the Arp2/3 complex links Cdc42-dependent signals to actin assembly. Cell *97*, 221–231.

Rohatgi, R., Nollau, P., Ho, H.Y., Kirschner, M.W., and Mayer, B.J. (2001). Nck and phosphatidylinositol 4,5-bisphosphate synergistically activate actin polymerization through the N-WASP-Arp2/3 pathway. J. Biol. Chem. *276*, 26448–26452.

Sallee, N.A., Rivera, G.M., Dueber, J.E., Vasilescu, D., Mullins, R.D., Mayer, B.J., and Lim, W.A. (2008). The pathogen protein EspF(U) hijacks actin polymerization using mimicry and multivalency. Nature *454*, 1005–1008.

Scita, G., Confalonieri, S., Lappalainen, P., and Suetsugu, S. (2008). IRSp53: Crossing the road of membrane and actin dynamics in the formation of membrane protrusions. Trends Cell Biol. *18*, 52–60.

Shevchenko, A., Chernushevich, I., Wilm, M., and Mann, M. (2000). De Novo peptide sequencing by nanoelectrospray tandem mass spectrometry using triple quadrupole and quadrupole/time-of-flight instruments. Methods Mol. Biol. *146*, 1–16.

Stradal, T.E., and Scita, G. (2006). Protein complexes regulating Arp2/3-mediated actin assembly. Curr. Opin. Cell Biol. *18*, 4–10.

Suetsugu, S., Murayama, K., Sakamoto, A., Hanawa-Suetsugu, K., Seto, A., Oikawa, T., Mishima, C., Shirouzu, M., Takenawa, T., and Yokoyama, S. (2006). The RAC binding domain/IRSp53-MIM homology domain of IRSp53 induces RAC-dependent membrane deformation. J. Biol. Chem. *281*, 35347–35358.

Swimm, A., Bommarius, B., Reeves, P., Sherman, M., and Kalman, D. (2004). Complex kinase requirements for EPEC pedestal formation. Nat. Cell Biol. *6*, 795.

Takenawa, T., and Suetsugu, S. (2007). The WASP-WAVE protein network: Connecting the membrane to the cytoskeleton. Nat. Rev. Mol. Cell Biol. *8*, 37–48.

Tian, L., Nelson, D.L., and Stewart, D.M. (2000). Cdc42-interacting protein 4 mediates binding of the Wiskott-Aldrich syndrome protein to microtubules. J. Biol. Chem. *275*, 7854–7861.

Trost, M., Wehmhoner, D., Karst, U., Dieterich, G., Wehland, J., and Jansch, L. (2005). Comparative proteome analysis of secretory proteins from pathogenic and nonpathogenic Listeria species. Proteomics *5*, 1544–1557.

Unsworth, K.E., Mazurkiewicz, P., Senf, F., Zettl, M., McNiven, M., Way, M., and Holden, D.W. (2007). Dynamin is required for F-actin assembly and pedestal formation by enteropathogenic Escherichia coli (EPEC). Cell. Microbiol. *9*, 438–449.

Westermeier, R., Barnes, N., Gronau-Czybulka, S., and Habeck, C. (1997). Electrophoresis in Practice, Second Edition (Weinheim: Wiley-VCH).

Yamagishi, A., Masuda, M., Ohki, T., Onishi, H., and Mochizuki, N. (2004). A novel actin bundling/filopodium-forming domain conserved in insulin receptor tyrosine kinase substrate p53 and missing in metastasis protein. J. Biol. Chem. *279*, 14929–14936.